Preparation and Performance of Poly(vinyl alcohol/ Nanofibrillated Cellulose/Sodium Tetraborate Hydrogels Based on Dynamic Borate Ester Bonds

Kehong Zhang ,* Xiaohu Zhu, Shufan Li, Minyi Wang, and Yue Zhang

A high-strength, tough, and self-healing hydrogel was fabricated using polyvinyl alcohol (PVOH) as the matrix, cellulose nanofibers (NFC) as the reinforcing agent, and sodium tetraborate (PB) as the crosslinking agent. The resulting PVOH/NFC/PB hydrogel has a dual-network structure formed by hydrogen bonds and dynamic borate ester bonds. The effects of NFC content on the hydrogel's mechanical, self-healing, water retention, and electrical properties were systematically investigated. Results showed that NFC addition markedly increased tensile strength, with a maximum value of 47.2 kPa achieved at 1.2 wt% NFC. The elongation at break reached its peak (1038.5%) at 0.8 wt% NFC. Owing to the presence of dynamic borate ester bonds, the hydrogel exhibited outstanding self-healing capability, achieving a healing efficiency of 94.6% within 60 s at 1.2 wt% NFC. Moreover, NFC content influences the hydrogel's water retention behavior and electrical conductivity, the latter reaching 0.345 S/m at 1.2 wt% NFC. The excellent plasticity and multifunctional properties of the PVOH/NFC/PB hydrogel highlight its promising potential for diverse applications.

DOI: 10.15376/biores.21.2.4235-4245

Keywords: Dynamic borate ester bond; Cellulose nanofibers; Hydrogel; Self-healing property

*Contact information: Anhui Engineering Research Center for Highly Functional Fiber Products for Automobiles, College of Materials and Chemistry, Anhui Agricultural University, Hefei, Anhui 230036, China; * Corresponding author: zkh@ahau.edu.cn*

INTRODUCTION

With the rapid development of flexible electronics and artificial intelligence, there is a growing demand for high-performance wearable sensors, electronic skins, and soft actuators (Wang *et al.* 2018; Ray *et al.* 2019). Hydrogels, characterized by their three-dimensional polymer networks and high-water content, have emerged as ideal candidates for these applications due to their excellent biocompatibility, tunable mechanical properties, and structural similarity to biological tissues (Yang *et al.* 2023). In emerging technologies, stimulus-responsive hydrogels are driving advances in flexible electronics and soft robotics (Du *et al.* 2024). Strain sensors containing hydrogels can monitor human movement in real time. Light-responsive hydrogel actuators can convert light energy into mechanical energy, enabling autonomous motion in micro-robots. However, conventional conductive hydrogels are susceptible to irreversible structural damage caused by mechanical fatigue or external forces during prolonged use, leading to the failure of electrical signal transmission and a shortened service life. Consequently, the development of conductive hydrogels with intrinsic self-healing capabilities—able to autonomously

restore their mechanical and electrical functions after damage—has become a critical focus in the field of material science.

To achieve self-healing properties, dynamic non-covalent interactions, such as hydrogen bonding, electrostatic interactions, and dynamic covalent bonds, are frequently introduced into the polymer matrix. Polyvinyl alcohol (PVOH) is a widely used water-soluble polymer for fabricating self-healing hydrogels owing to its abundance of hydroxyl groups. Conventional preparation methods primarily include physical crosslinking (*e.g.*, freeze-thaw cycles) and chemical crosslinking (*e.g.*, boric acid, glutaraldehyde). Physical crosslinking creates networks through intermolecular hydrogen bonds and microcrystalline structures, offering excellent biocompatibility but limited mechanical strength (Sasaki *et al*. 2016). Chemical crosslinking improves structural stability by introducing covalent bonds, yet it may result in residual toxic agents (Dai *et al*. 2025). Consequently, novel crosslinking strategies are being actively developed to overcome these limitations. A classic strategy involves crosslinking PVOH with borax (sodium tetraborate decahydrate). In aqueous solutions, borax dissociates into borate ions, which form dynamic reversible borate ester bonds (di-diol complexes) with the hydroxyl groups on PVOH chains. These dynamic bonds can readily break and reform in response to external stimuli, endowing the hydrogel with rapid self-healing and remodeling abilities at room temperature. Furthermore, the free ions generated from borax provide the hydrogel with ionic conductivity, making the PVOH/Borax system a promising platform for sensing applications. Leveraging the synergistic effects of dynamic borate ester bonds and hydrogen bonds, Shi *et al.* (2025) developed conductive hydrogels capable of rapidly releasing carriers at a low voltage of 1.5 V, thereby circumventing the stability issues associated with conventional redox reactions. Zou *et al.* (2023) employed the Hofmeister effect to induce self-assembly of PVOH chains, in combination with the ionic hydration of inorganic salts, to fabricate a strong and tough hydrogel exhibiting a tensile strength of 25.02 MPa and low-temperature tolerance down to −47.6 °C. Cheng *et al.* (2023) developed a highly stretchable self-healing hydrogel with dual cross-linking network through borate ester bonds generated by polyvinyl alcohol and borax, and acylhydrazone bonds formed by aldehyde nanocellulose with adipic acid dihydrazide-modified alginate. The hydrogel can monitor both large and subtle human motions.

Despite these advantages, pure PVOH/borax hydrogels often suffer from poor mechanical strength and dimensional stability, thus limiting their practical application in scenarios requiring durability and toughness. To overcome these limitations, incorporating reinforcing nanofillers into the hydrogel network has proven to be an effective strategy. Nanofibrillated cellulose (NFC, also called CNF), a sustainable nanomaterial derived from natural resources, possess high aspect ratios, exceptional mechanical stiffness, and a high population of surface hydroxyl groups. The introduction of NFC into the PVOH matrix not only can serve as a physical skeleton to reinforce the hydrogel but also participate in the formation of multiple dynamic interactions—including hydrogen bonds between NFC and PVOH, and borate ester bonds with the borate ions. This synergistic effect is expected to significantly enhance the mechanical robustness of the hydrogel without compromising its self-healing efficiency. This work reports a facile and effective strategy to fabricate a self-healing, mechanically robust, and conductive composite hydrogel based on the PVOH/NFC/borax system. By leveraging the dynamic crosslinking network formed by borax and the reinforcing effect of NFC, the resulting hydrogel exhibits excellent self-healing performance and enhanced mechanical properties. The structure–property relationships, including mechanical behavior, healing kinetics, and conductivity recovery,

are systematically investigated to provide insights for designing next-generation multifunctional soft materials.

EXPERIMENTAL

Materials

Polyvinyl alcohol (PVOH) with an average polymerization degree of 1750 ± 50 was purchased from Shanghai Aladdin Biochemical Technology Co., Ltd. (Shanghai, China). The nano-cellulose suspension NFC-B5 (NFC) was provided by Zhejiang Jinjiahao Green Nanomaterials Co., Ltd. (Quzhou, China), with a mass fraction of 10 wt%, a diameter of 3 to 30 nm, and a length of 50 to 300 nm. Sodium tetraborate decahydrate ($Na_2B_4O_7 \cdot 10H_2O$; PB) was purchased from Xilong Chemical Co., Ltd. (Shantou, China). All reagents were of analytical grade and were not further purified for use.

Preparation of PVOH/NFC/PB Hydrogel

A NFC suspension with a mass fraction of 10 wt% was poured into a beaker, and deionized water was added. After stirring evenly with a glass rod, it was ultra-sonically dispersed for 30 min using a KQ-100DA CNC ultrasonic cleaning machine (Kun Shan Ultrasonic Instruments Co., Ltd) to produce a 5 wt% NFC suspension, which was then set aside for later use. A 2 wt% $Na_2B_4O_7$ solution (PB) was pre-pared by dissolving $Na_2B_4O_7 \cdot 10H_2O$ in deionized water. A certain amount of 5 wt% NFC suspension was diluted with deionized water to a total volume of 84 mL, then 6 g of PVOH was added. The mixture was stirred at 90 °C for 2 h in a DF-101S magnetic stirrer (Changzhou Guoyu Instrument Manufacturing Co., Ltd.) to prepare the PVOH/NFC solution. Then, a 2 wt% PB solution was added to the cooled PVOH/NFC mixture solution until the total volume reached 100 mL. The mixture solution was heated and stirred in a 75 °C water bath to form a gel, which was then poured into a petri dish and vacuum-dried at 70 °C for 30 min to pre-pare the PVOH/NFC/PB hydrogel. The prepared PVOH/NFC/PB hydrogel is denoted as PVOH-x/NFC-y/PB-z based on the mass fractions x%, y%, and z% of PVOH, NFC, and PB in the hydrogel.

Characterizations

Over the range of 400 to 4000 cm^{-1}, the absorbance spectra of all samples were collected using a TENSOR II infrared spectrometer (Bruker Corporation, Karlsruhe, Germany) through 32 scans at a resolution of 4 cm^{-1}. The tensile properties of the samples were evaluated with dumbbell-shaped specimens using an Instron3400 mechanical testing systems (Instron Corporation, Boston, USA) with the tensile speed of 50 mm/min (the length × width × thickness of samples was 50 mm × 4 mm × 2 mm). The results for mechanical properties were reported as the average of 5 samples. The dumbbell-shaped PVOH/NFC/PB hydrogel samples were uniformly cut into two halves, and then the broken ends were quickly joined together without applying pressure to allow the hydrogel to heal. The self-healing properties of the hydrogel were tested using an Instron3400 mechanical testing systems (Instron Corporation, Boston, USA) with the tensile speed of 50 mm/min after 10 s, 30 s, and 60 s of self-healing. The self-healing properties were the average of 3 samples. The hydrogels were cut into small pieces of a certain mass and placed in a constant temperature drying oven DZF-6050 (Shanghai Yiheng Technology Instrument Co., Ltd., China) at 70 °C. The mass was weighed every hour and recorded as m. The water retention

property of the hydrogel was evaluated by calculating $(m_0 - m)/m_0 \times 100\%$, where m_0 is the initial mass of the sample and m is its mass after a specific time interval. After sandwiching the hydrogel sample between two graphite plates, wrapping it with plastic wrap, and leaving space for the electrical connection (the length × width × thickness of samples was 20 mm × 20 mm × 2 mm), the conductivity was tested using CHI760E electrochemical workstation (Shanghai Chenhua Instrument Co., Ltd., China). The conductivity properties were the average of 3 samples. To demonstrate the plasticity of the hydrogel, the PVOH-6/NFC-1.2/PB-2 hydrogel was selected as the object. Before the hydrogel completely cooled down, it was placed in molds of different shapes and extruded. After cooling, it was taken out to observe its molding ability.

RESULTS AND DISCUSSION

FTIR Analysis

Figure 1 shows the FTIR spectra of PVOH, PVOH-6/NFC-1.2/PB-0 and PVOH-6/NFC-1.2/PB-2. The FTIR spectrum of PVOH exhibited characteristic absorbance peaks at 3300 cm^{-1} (–OH stretching), 2920 cm^{-1} (–CH_2 stretching), 1429 cm^{-1} (–CH_2 bending), and 1090 cm^{-1} (–C–O–C– stretching). Compared with the infrared spectrum of PVOH, the characteristic peak at 3300 cm^{-1} in the spectra of PVOH-6/NFC-1.2/PB-0 and PVOH-6/NFC-1.2/PB-2 was enhanced, indicating that the addition of NFC promoted intertwining between PVOH and NFC chains and strengthened hydrogen bonding among hydroxyl groups. Relative to PVOH and PVOH-6/NFC-1.2/PB-0, the spectrum of PVOH-6/NFC-1.2/PB-2 showed the disappearance of the characteristic peaks at 2920 cm^{-1} and 2852 cm^{-1} associated with PVOH and NFC, while a new peak emerged at 1640 cm^{-1}. This suggests that the introduction of $Na_2B_4O_7$ resulted in the appearance of typical characteristic peaks of $Na_2B_4O_7$ and borate in the hydrogel. The absorbance peak at 1640 cm^{-1}, corresponding to B-O-C, indicates that the hydroxyl groups of PVOH and NFC react with $Na_2B_4O_7$ to form dynamic borate ester bonds, endowing the hydrogel with self-healing properties.

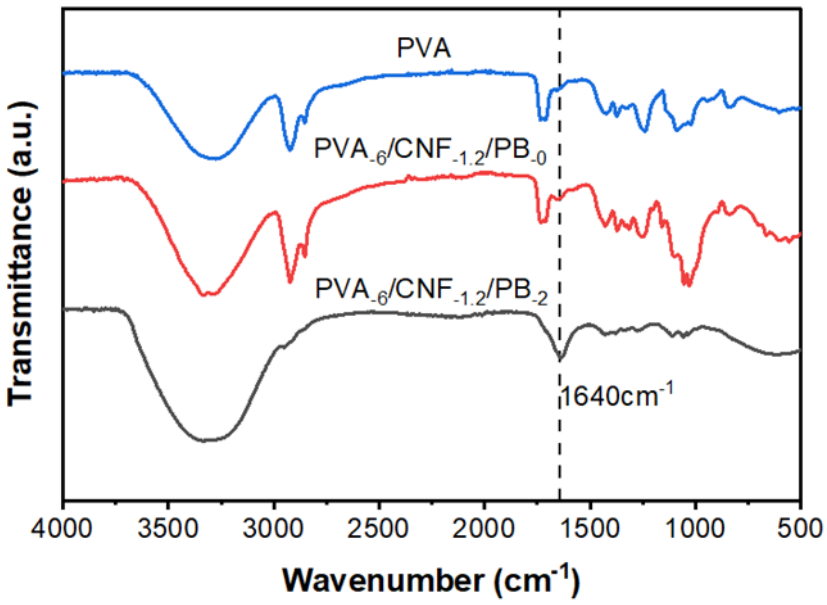

Fig. 1. FTIR spectra of PVOH, PVOH-6/NFC-1.2/PB-0 and PVOH-6/NFC-1.2/PB-2 hydrogels

SEM Analysis

To investigate the influence of the NFC content on the morphology of the hydrogel, the samples of PVOH-6/NFC-0/PB-2, PVOH-6/NFC-0.4/PB-2, and PVOH-6/NFC-1.2/PB-2 were observed by SEM. As for PVOH-6/NFC-0/PB-2, it was obvious that the overall structure was porous and sponge-like, with a large amount of honeycomb pores evenly distributed throughout the hydrogel (Fig. 2a). Compared with PAVA-6 /NFC-0/PB-2, the microstructure of PAVA-6 /NFC-0.4/PB-2 changed significantly with the introduction of NFC. The pore sizes within PVOH-6/NFC-0.4/PB-2 were large and varied in size, and a great number of small pores were observed inside the large pores, as shown in Fig. 2b. The interconnection of NFC and PVOH created the large pores structure within the hydrogel. On the pore walls of these large pores, the interweaving and entanglement of NFC nanofibers led to the formation of smaller pores. Furthermore, a denser network with thick walls, small size and uniform pores was observed for the PVOH-6/NFC-1.2/PB-2 hydrogel when the amount of NFC was increased from 0.4 g to 1.2 g, owing to the increase of cross-linking density (Fig. 2c).

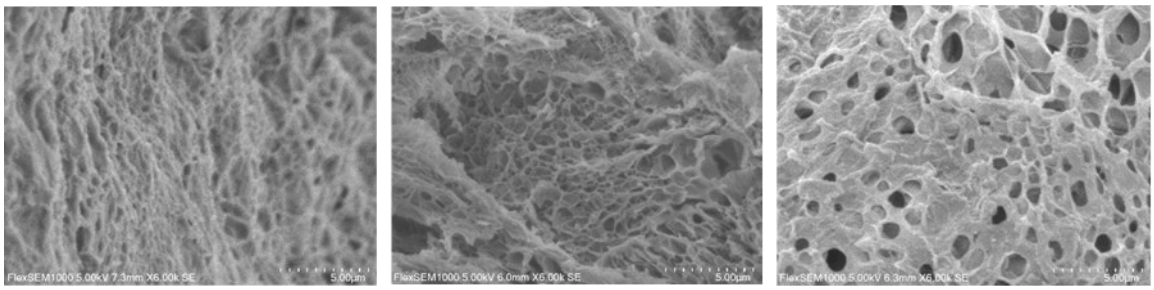

(a) PVOH-6/NFC-0/PB-2 **(b)** PVOH-6/NFC-0.4/PB-2 **(c)** PVOH-6/NFC-1.2/PB-2

Fig. 2. The SEM images of PVOH-6/NFC-y/PB-2 hydrogels with different NFC content

Mechanical Properties

Mechanical properties are crucial indicators for evaluating hydrogel performance. The tensile strength and elongation at break of PVOH-6/NFC-y/PB-2 hydrogels with different NFC content, along with their strain-stress curves, are presented in Fig. 3, where y = 0, 0.4, 0.8, 1.2, and 1.6.

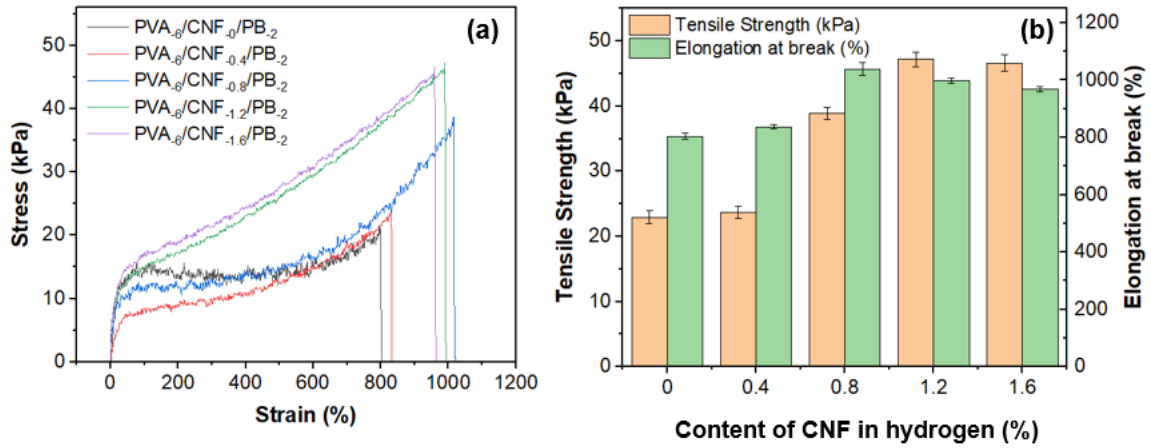

Fig. 3. (a) The strain-stress curves of PVOH-6/NFC-y/PB-2 hydrogels (y = 0,0.4,0.8,1.2,1.6); (b) the tensile properties of PVOH-6/NFC-y/PB-2 hydrogels with different NFC content

Clearly, the mechanical properties of PVOH/NFC/PB hydrogels were strongly influenced by the NFC content. The incorporation of NFC enhanced the tensile strength of the hydrogels. As a rigid reinforcing agent, NFC formed cross-links with PVOH through dynamic borate ester bonds in the presence of PB. Simultaneously, it established hydrogen bonds with PVOH, thereby improving both tensile strength and elongation at break. At a NFC content of 1.2 wt%, the tensile strength reached a maximum of 47.2 kPa, representing a 106% increase over hydrogels without NFC.

The elongation at break peaked at an NFC content of 0.8 wt%, reaching 1040%, which was a factor of 0.29 increase compared to the NFC-free hydrogel. Beyond a certain NFC content, NFC agglomeration within the PVOH limits tensile strength and decreased elongation at break of the hydrogel.

Self-healing Properties

Figure 4 shows the self-healing property of the PVOH/NFC/PB hydrogel. Figure 4(a-b) illustrates the self-healing property of the PVOH-6/NFC-1.2/PB-2 hydrogel at different self-healing times. As the self-healing time increased, the tensile strength of the hydrogel continuously increased. When the self-healing time was 60 seconds, the self-healing efficiency reached 94.6%. However, the elongation at break of the hydrogel exhibited a trend of first increasing and then decreasing. The combined effects of hydrogen bonds and dynamic borate ester bonds enabled the hydrogel to re-heal at the cut site after being severed.

As the self-healing time increased, more hydrogen bonds and dynamic borate ester bonds were regenerated, thereby increasing the tensile strength of the self-healed hydrogel. However, the continuous loss of water in the hydrogel led to a decrease in the elongation at break.

Figure 4(c-d) shows the mechanical properties of PVOH/NFC/PB hydrogels with different NFC contents after 30 seconds of self-healing. It can be observed that both the tensile strength and elongation at break of the self-healing hydrogels increased first and then decreased with the increase of NFC content. When the NFC content reached 1.2 wt%, the tensile strength and elongation at break of the self-healing hydrogel attained their maximum values.

At low NFC contents, the number of hydrogen bonds and dynamic borate ester bonds at the hydrogel incision interface increased with NFC content, enhancing the hydrogel's tensile strength. Simultaneously, freely diffusible PVOH molecular chains at the incision interface enhanced the hydrogel's healing efficacy and elongation at break. However, high NFC content led to the formation of a rigid percolation network, which greatly restricted the free movement ability of PVOH molecular chains. With the increase of NFC, the viscosity of the hydrogel system rose sharply. The PVOH molecular chains at the cut interface had difficulty in diffusing to the opposite side and entangling with each other.

This restricted diffusion also prevented rapid reconstruction of borate bonds and hydrogen bonds at the incision site. Consequently, during stretching, the hydrogel fractured directly at poorly healed incisions, which was manifested as simultaneous reductions in both strength and elongation. Figure 5 illustrates the self-healing process of PVOH hydrogel.

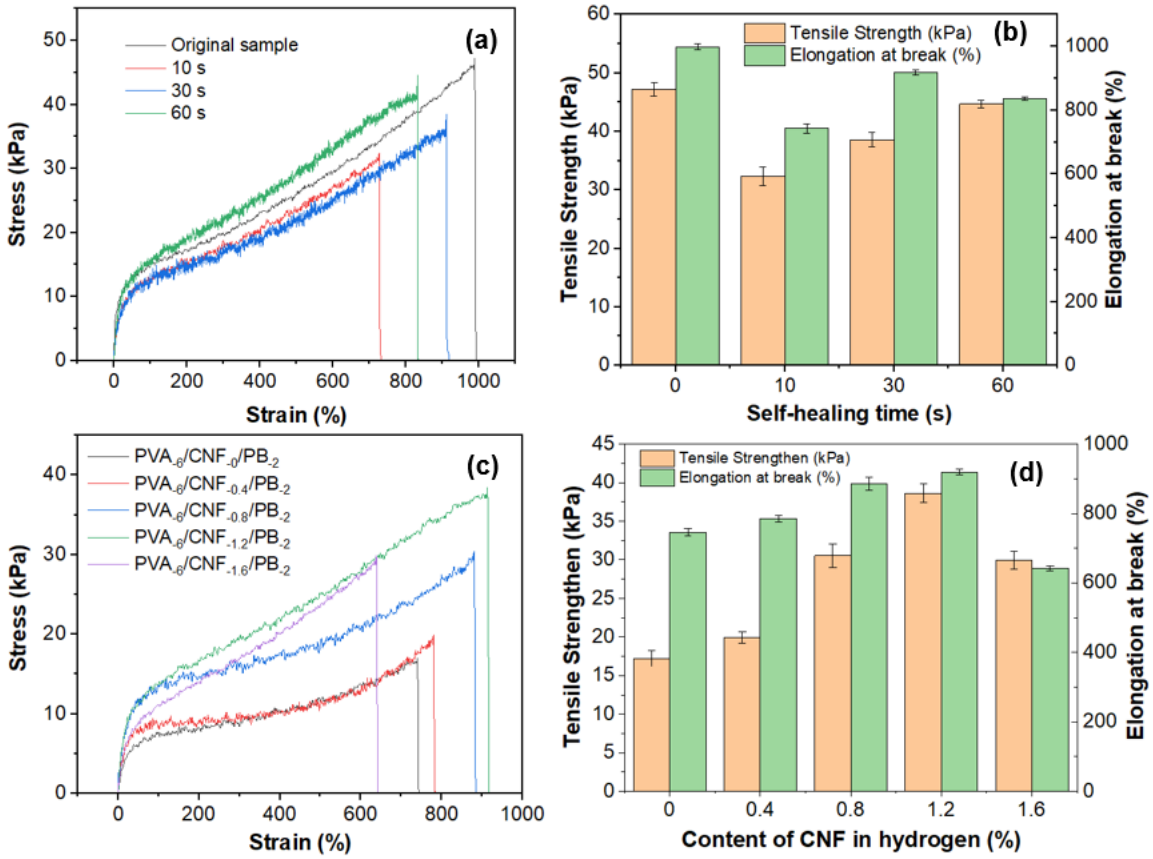

Fig. 4. The strain-stress curves (a) and the tensile properties (b) of PVOH-6/NFC-y/PB-2 hydrogels under different self-healing times; the strain-stress curves (c) and the tensile properties (d) of PVOH-6/NFC-y/PB-2 hydrogels (y = 0,0.4,0.8,1.2,1.6) at a self-healing time of 30 s

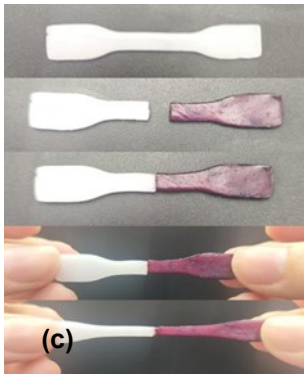

Fig. 5. Self-healing process of PAVA-6 /NFC-1.2/PB-2 hydrogel

Water Retention Property

Figure 6 shows the water retention property of PVOH/NFC/PB hydrogels with different NFC content. The content of NFC directly affects the water loss of the hydrogel. Hydrophilic NFC, rich in hydroxyl groups (–OH), forms hydrogen bonds with water molecules, enhancing the hydrogel's water absorption capacity. Moreover, NFC improves the pore structure of the PVOH network, generating additional micropores that help retain moisture and slightly enhance water retention. The water loss, a key indicator of the

hydrogel's moisture retention performance, increased initially at a faster rate and then slowed down as drying time increased. Increasing the NFC content reduced the water loss rate of the PVOH-6/NFC-y/PB-2 hydrogel. PVOH and NFC form dynamic borate ester bonds through reaction with PB, creating a more tightly semi-interpenetrating network (semi-IPN). The synergistic effect of physical crosslinking (hydrogen bonds) and chemical crosslinking (semi-IPN) enhances the mechanical strength and network stability of the hydrogel. The pore size distribution of the hydrogel becomes more uniform, increasing water migration resistance and significantly improving water retention. The high crystallinity of NFC may further inhibit water diffusion. Overall, the PVOH-6/NFC-y/PB-2 hydrogel exhibited optimal water retention at a NFC content of 1.2 wt%.

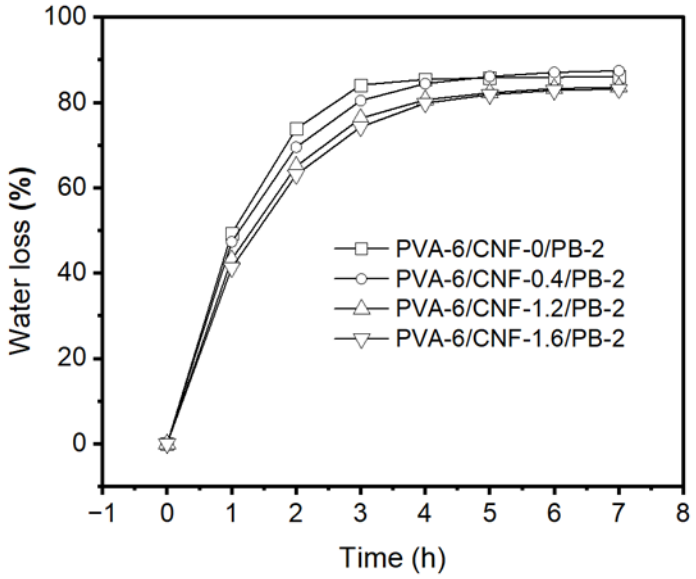

Fig. 6. The water retention properties of PVOH/NFC/PB hydrogels

Conductivity Property

Figure 7 shows the conductivity of PVOH-6/NFC-y/PB-2 hydrogels with different NFC contents. Increasing the NFC content in the hydrogel enhanced the conductivity of the PVOH-6/NFC-y/PB-2 hydrogel, but the increase in conductivity diminished. The conductivity of the PVOH-6/NFC-y/PB-2 hydrogel originates from the ions released upon the dissolution of PB. These ions serve as the primary carriers for the conductivity of PVOH-6/NFC-y/PB-2 hydrogels. The NFC added to PVOH, with its nanofiber morphology and abundant surface hydroxyl groups, pre-organized the arrangement of PVOH chains through hydrogen bonds, preventing the aggregation of PVOH. This enabled the subsequent borax cross-linking reaction to occur more uniformly, thereby forming a three-dimensional network with fewer defects and uniform pore sizes. This uniform and hydrophilic network structure provided continuous and low-resistance transmission channels for ions such as Na^+ and BO_3^{3-}, thus promoting ion transport. Part of the hydroxyl groups (-OH) on the NFC surface can assist ion transport through a hydrogen bond network, thereby enhancing conductivity. Meanwhile, water molecules can serve as ion transport media.

As the NFC content increased, it is hypothesized that the semi-interpenetrating network (semi-IPN) formed by NFC and PVOH under the action of PB enhanced the water absorption of the hydrogel, thereby improving its ionic conductivity. Additionally, the

microchannels formed by NFC in the hydrogel are expected to facilitate the directed transport of electrolyte ions (such as Na^+ and $[B(OH)_4]^-$ from the dissociation of PB). However, as the NFC content continued to increase, excessive NFC may lead to phase separation or aggregation, disrupting the continuity of the PVOH network and hindering ion transport, resulting in a plateau or even a decrease in conductivity.

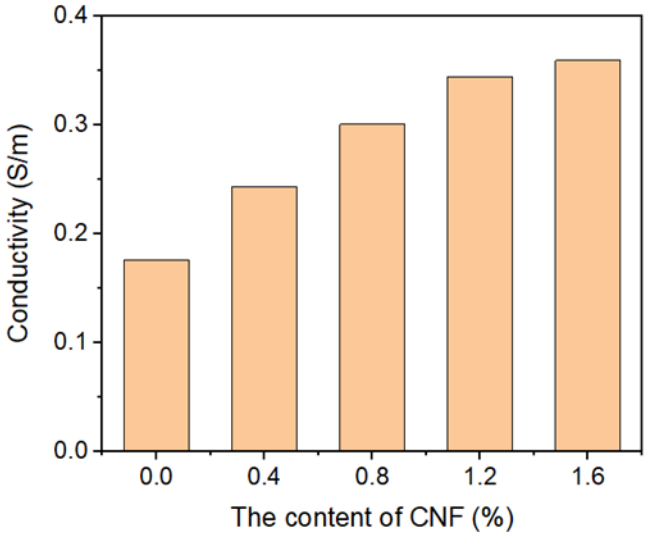

Fig. 7. The conductivity property of PVOH-6/NFC-y/PB-2 hydrogels with different NFC content (y = 0,0.4,0.8,1.2,1.6)

Plasticity Analysis

Evidence of the plasticity of PVOH/NFC/PB hydrogels is shown in Fig. 8. Using molds, the PVOH-6/NFC-1.2/PB-2 hydrogel was shaped into various forms such as square, flower, star, circle, and triangle. The shaped PVOH/NFC/PB hydrogel objects maintained their shape stability over an extended period. This demonstrates that the PVOH/NFC/PB hydrogel possessed excellent plasticity and shaping capability. The internally structured PVOH/NFC/PB hydrogel exhibited a uniform internal structure with no noticeable layering or defects.

A uniform internal structure is a prerequisite for good plasticity, ensuring that deformation or cracking does not occur during shaping due to inconsistent internal structure. The excellent plasticity of hydrogels enables their application in various fields, such as drug delivery systems or tissue engineering scaffolds in the biomedical field, and sensors or electrodes with specific shapes in the flexible electronics field.

Fig. 8. Plasticity of PAV-6 /NFC-1.2/PB-2 hydrogel

CONCLUSIONS

1. A high-strength, high-toughness poly(vinyl alcohol)/nanofibrillated cellulose/sodium borate (PVOH/NFC/PB) self-healing hydrogel was developed with PVOH as the matrix, NFC as the reinforcing agent, and PB as the crosslinking agent. The hydrogel featured a dual network structure formed by hydrogen bonds and dynamic borate ester bonds.
2. The dynamic borate ester bonds were formed between PVOH and NFC by reacting with PB. The Fourier transform infrared (FTIR) spectrum of the PVOH/NFC/PB hydrogel showed an absorbance peak at 1640 cm^{-1}, corresponding to B-O-C, confirming the formation of the borate ester bonds and endowing the hydrogel with self-healing properties.
3. The introduction of NFC enhanced the tensile strength of the hydrogel. At a NFC content of 1.2 wt%, the tensile strength of the PVOH/NFC/PB hydrogel reached 47.2 kPa. The maximum elongation at break of 1040% was achieved at an NFC content of 0.8 wt%. The presence of dynamic borate ester bonds enabled PVOH/NFC/PB hydrogels to exhibit excellent self-healing properties. At a NFC content of 1.2 wt%, the self-healing efficiency of the PVOH/NFC/PB hydrogel within 60 seconds reached 94.6%.
4. The water retention performance and conductivity of PVOH/NFC/PB hydrogels were also affected by the content of NFC. At a NFC content of 1.2 wt%, the electrical conductivity of the hydrogel reached 0.345 S/m. The PVOH/NFC/PB hydrogels exhibited excellent plasticity.

ACKNOWLEDGMENTS

The authors are grateful for the support of the Natural Science Research Project of Anhui Educational Committee, Grant No. 2023AH050979; the Anhui Agricultural University-Anhui Huayi Packaging Technology Co. Ltd. cooperation project, Grant No. hx23402; and Anhui Agricultural University College Students Innovation and Entrepreneurship Training Program, Grant Nos. S202310364142, and S202310364153.

REFERENCES CITED

Cheng, H., Fan, Z., Wang, Z., Guo, Z., Jiang, J., and Xie, Y. (2023). "Highly stretchable, fast self-healing nanocellulose hydrogel combining borate ester bonds and acylhydrazone bonds," *Int. J. Biol. Macromol* 245, article 125471. https://doi.org/10.1016/j.ijbiomac.2023.125471

Dai, S., Zhong, C., Yao, J., Zeng, L., Zhong, Y., Xie, S., Huang, W., Chen, W., and Sui, Y. (2025). "High-strength and low-hysteresis chemical cross-linking PVOH hydrogel for motion monitoring," *Colloid Surface A* 710, article 136212. https://doi.org/10.1016/j.colsurfa.2025.136212

Du, F., Wang, S., Chen, Z., and Li, Q. (2024). "Stimuli responsive actuators: Recent advances," *J. Mater. Chem. C* 12(23), 8217-8242. https://doi.org/10.1039/D4TC00911H

Ray, T. R., Choi, J., Bandodkar, A. J., Krishnan, S., Gutruf, P., Tian, L., Ghaffari, R., and Rogers, J. A. (2019). "Bio-integrated wearable systems: A comprehensive review," *Chem. Rev.* 119(8), 5461-5533. https://doi.org/10.1021/acs.chemrev.8b00573

Sasaki, S., Murakami, T., and Suzuki, A. (2016). "Frictional properties of physically cross-linked PVOH hydrogels as artificial cartilage," *Biosurface and Biotribology* 2(1), 11-17. https://doi.org/10.1016/j.bsbt.2016.02.002

Shi, Y., Tang, Z., Li, C., Miao, Y., Zhu, L., and Yue, B. (2025). "Conductive hydrogel systems enabling rapid and controllable release of guests at low-voltage region," *Small* 21(7), article 2410120. https://doi.org/10.1002/smll.202410120

Wang, S., Oh, J. Y., Xu, J., Tran, H., and Bao, Z. (2018). "Skin-inspired electronics: an emerging paradigm," *Acc. Chem. Res.* 51(5), 1033-1045. https://doi.org/10.1021/acs.accounts.8b00015

Yang, J., Chen, Y., Zhao, L., Zhang, J., and Luo, H. (2023). "Constructions and properties of physically cross-linked hydrogels based on natural polymers," *Polym. Rev.* 63(3), 574-612. https://doi.org/10.1080/15583724.2022.2137525

Zou, H., Meng, X., Zhao, X., and Qiu, J. (2023). "Hofmeister effect-enhanced hydration chemistry of hydrogel for high-efficiency solar-driven interfacial desalination," *Adv. Mater.* 35(5), article 2207262. https://doi.org/10.1002/adma.202207262

Article submitted: August 14, 2025; Peer review completed: October 11, 2025; Revised version received: Dec. 4, 2026; Accepted: March 11, 2026; Published: March 27, 2026.
DOI: 10.15376/biores.21.2.4235-4245